Cancer Management and Research

Dovepress

open access to scientific and medical research

Open Access Full Text Article

ORIGINAL RESEARCH

Knockdown of circPRKCA Restrained Cell Growth, Migration, and Invasion of NSCLC Cells Both in vitro and in vivo via Regulating miR-330-5p/PDK1/AKT Pathway

This article was published in the following Dove Press journal:
Cancer Management and Research

Lanxiang Bai[1,*]
Xiaonu Peng[2,*]
Ruimei Sun[3]

[1]Disinfection Supply Center, Yantai Yuhuangding Hospital, Yantai 264000, Shandong, People's Republic of China; [2]Department of Thoracic Surgery, Yantai Yuhuangding Hospital, Yantai 264000, Shandong, People's Republic of China; [3]Department of Laboratory, Weifang No.2 People's Hospital, Weifang 261041, Shandong, People's Republic of China

*These authors contributed equally to this work

Background: Protein kinase Cα (PRKCA) is an oncogene in multiple cancers including non-small-cell lung cancer (NSCLC) and can be transcribed into a number of circular PRKCAs (circPRKCAs). Here, we aimed to elaborate the role and mechanism of circPRKCA_024 (circPRKCA) in malignant progression of NSCLC.

Methods: Expression of circPRKCA, miRNA (miR)-330-5p and 3-phosphoinositide-dependent protein kinase-1 (PDK1) was measured by real-time quantitative PCR and Western blotting, and their relationship was testified by dual-luciferase reporter assay, RNA immunoprecipitation, and RNA pull-down assay. Cell behaviors were evaluated by cell counting kit (CCK)-8, flow cytometry, and transwell assays. AKT activity was confirmed by Western blotting. Xenograft experiment assessed tumor growth.

Results: Expression of circPRKCA and PDK1 was upregulated, and miR-330-5p was downregulated in NSCLC tissues and cell lines. High circPRKCA was correlated with TNM stage and lymph node metastasis of NSCLC patients. Silencing circPRKCA could suppress cell viability, migration, and invasion in A549 and H1299 cells, accompanied with apoptosis rate promotion. Moreover, circPRKCA knockdown retarded tumor growth of A549 cells in vivo. Molecularly, miR-330-5p was sponged by circPRKCA, and PDK1 was a target of miR-330-5p. Inhibiting miR-330-5p could attenuate the suppression of circPRKCA knockdown on cell growth, migration, and invasion; contrarily, promoting miR-330-5p caused inhibition on those cell behaviors by downregulating PDK1. Analogously, AKT activity was suppressed by circPRKCA downregulation and miR-330-5p upregulation in NSCLC cells both in vitro and in vivo.

Conclusion: Depleting circPRKCA inhibited PDK1 to suppress NSCLC cell malignant behaviors through miR-330-5p/PDK1/AKT pathway.

Keywords: circPRKCA, miR-330-5p, PDK1, AKT, NSCLC

Introduction

Non-small-cell lung cancer (NSCLC) is the most prevailing type of lung cancer according to histological classification, and NSCLC is a devastating disease with a poor prognosis.[1] Most patients with NSCLC are diagnosed in late stages (III–IV) due to being asymptomatic at the early stages (I–II),[2] making it incurable despite receiving surgical resection, chemotherapy, and targeted therapy.[3] The morbidity and mortality in NSCLC are always ascribed to resistance, metastasis,

Correspondence: Ruimei Sun
Email sunruimeiweifang@163.com

and reoccurrence after therapy.[4] Furthermore, phosphoinositide 3-kinase (PI3K)/AKT signaling, a key pro-survival pathway in cancer cells, has been proposed as an attractive target for novel anticancer therapies in NSCLC.[5–7] Therefore, identifying novel biomarkers that target the PI3K/AKT pathway is of great importance to better understand the malignant development of NSCLC.

Circular RNAs (circRNAs) are a cluster of endogenous, single-stranded RNAs with a closed structure.[8] The circRNAs are stable and abundant in cells, as well as circulating fluids, such as blood. Thus, circRNAs are considered as novel promising biomarkers for human diseases including malignant pathologies.[9] The molecular mechanism of circRNAs includes acting as microRNA (miRNA) sponges or competing endogenous RNAs (ceRNAs) to regulate hallmarks of cancer.[10]

Research on circRNA in lung cancer has been on the rise, and plenty of circRNAs are demonstrated to be deregulated in tissue biopsies and liquid biopsies of NSCLC patients.[11,12] Protein kinase Cα (PRKCA) is a member of the PKC family which has been implicated in various cellular functions.[13] PRKCA is an oncogene in multiple cancers including lung cancer, and is highly expressed in about 20% of NSCLC patients.[14,15] The PRKCA gene can be transcribed into a number of circular PRKCAs (circPRKCAs) including hsa_circPRKCA_024 (hsa_circRNA_102179; hsa_circ_0007580′ also named as circPRKCA). According to the GSE112214 database, circPRKCA is upregulated in NSCLC tumor tissues. However, the role and mechanism of circPRKCA in NSCLC cells remain to be expounded.

MiRNAs are another type of small, linear noncoding RNAs with about 22 nucleotides. The roles of miRNAs have been well-documented in lung cancer carcinogenesis and behaviors, as well as the diagnosis and prognosis.[16] MiRNA (miR)-330-5p is downregulated in multiple malignant tumors, such as glioblastoma, colorectal cancer, prostate cancer,[17–19] and NSCLC as well.[20] The 3-phosphoinositide-dependent protein kinase-1 (PDK1), one crucial node of the PI3K pathway, can physically phosphorylate AKT.[21] Moreover, PDK1 is a key oncogene to promote NSCLC cell growth and metastasis.[22] Therefore, in this study, we intended to investigate the expression and role of circPRKCA, miR-330-5p, and PDK1 in human NSCLC cells.

Materials and Methods

Tissue Specimens

Study participants included 51 patients diagnosed with NSCLC in Yantai Yuhuangding Hospital. These patients were histopathologically verified to bear primary NSCLC tumors from Stage I to IV, and received no local or systemic chemoradiotherapy before their surgery. The clinicopathological characteristics of these patients are summarized in Table 1, such as gender, age, smoke, histological type, tumor nodes metastasis (TNM) stage, and lymph node metastasis. The tumor tissues and adjacent normal tissues (≥5 cm from tumor tissues) were collected after informed written consent documents from every patient were obtained. This study was approved by the Ethics Committee of Institutional Research of Yantai Yuhuangding Hospital.

Cell Culture and Transfection

Two NSCLC cell lines A549 (no. 10185) and H1299 (no. 25803) were from the Korean Cell Line Bank (Seoul National University College of Medicine; Yongon-dong, Chongno-gu, Seoul, Korean), and one normal lung

Table 1 Association of circPRKCA Expression in Non-Small-Cell Lung Cancer (NSCLC) Patients with Different Clinicopathological Characteristics

Clinicopathological Characteristics	Number	circPRKCA		*P*
		High (30)	Low (21)	
Gender				0.063
Female	21	12	9	
Male	30	18	12	
Age (years)				0.077
<50	25	16	9	
≥50	26	14	12	
Smoking				0.059
Non-smokers	24	14	10	
Smokers	27	16	11	
Histological type				0.054
Well, moderate	22	13	9	
Poor	29	17	12	
TNM stage				0.0015
I–II	23	7	16	
III	28	23	5	
Lymph node metastasis				0.012
Negative	24	8	16	
Positive	27	22	5	

Abbreviation: TNM, tumor nodes metastasis.

bronchial epithelium cell line BEAS-2B (no. 95102433) was from European Collection of Authenticated Cell Cultures (Public Health England; Salisbury, UK). All the cells were cultured in Roswell Park Memorial Institute (RPMI)-1640 medium (Gibco, Grand Island, NY, USA) with 10% inactivated fetal bovine serum (FBS; Gibco). The oligonucleotides including siRNAs against circPRKCA (si-circPRKCA#1, si-circPRKCA#2, and si-circPRKCA#3), miR-330-5p mimic, and miR-330-5p inhibitor (in-miR-330-5p) were bought from GenePharma (Shanghai, China), as well as their negative controls (si-NC, miR-NC mimic, and in-miR-NC). To overexpress PDK1, the pcDNA 3.1 (+) vector (pcDNA) was purchased from Invitrogen (Carlsbad, CA, USA), and the coding domain sequence of PDK1 was cloned into pcDNA. For cell transfection, 40 nM of oligonucleotides and 2 μg vectors were separately transfected into A549 and H1299 cells using Lipofectamine 2000 (Invitrogen) according to the instructions. The sequence of oligonucleotides is presented in Table 2.

Real-Time Quantitative PCR (RT-qPCR) and Western Blotting

The total RNA in tissues and cells was extracted by Trizol (Invitrogen), and was subsequently reverse-transcribed to cDNA according to the manufacturer's protocol. The RT-qPCR reaction was performed using SYBR Premix Ex Taq™ (Takara, Tokyo, Japan) and primers on ABI 7500 version with a fast real-time PCR system. The sequence of primers are listed in Table 3, and β-actin (for circPRKCA and PDK1 mRNA) and U6 (for miR-330-5p) were served as the built-in controls. The reaction system of each gene was performed in quadruplicate, and the relative gene expression level was calculated using $2^{-\Delta\Delta Ct}$ method prior to normalization to control groups.

The total protein in tissues and cells was isolated using NP-40 lysis buffer (Beyotime, Shanghai, China), and was subsequently experienced normal Western blotting procedures as previous study.[23] The antibodies were from Abcam (Cambridge, UK) and are listed in Table 4, and immunoreactive signals were detected by enhanced chemiluminescence (ECL) technique

Table 3 The RT-qPCR Primers Used in This Study

Gene	Primer Sequence (5′-3′)
circPRKCA	ATATCGCCCCAGAGAAAGCC GGCAAGCATCACCTTTCCAA
miR-330-5p	TCTCTGGGCCTGTGTCTTAGGC TTAATGGGGTGATTGGTGGT
PDK1	GGAGGAGGACGCTGAGGAG GCAGGAACATAACACCACGC
β-actin	CACAGAGCCTCGCCTTTGCC ACCCATGCCCACCATCACG
U6	GTGCTCGCTTCGGCAGCACATATAC AAAAATATGGAACGCTTCACGAATTTG

Table 2 The Oligonucleotides Used in This Study for Transfection

Gene	Sequence (5′-3′)
si-circPRKCA#1	CGGACUUCAAUUUCCUCAUGG AUGAGGAAAUUGAAGUCCGUG
si-circPRKCA#2	GAUUCAGAAGGACAUAUCAAA UGAUAUGUCCUUCUGAAUCCA
si-circPRKCA#3	GGAUUGUUCUUUCUUCAUAAA UAUGAAGAAAGAACAAUCCGA
si-NC	GCUACGAUCUGCCCAAGAUTT AUCUUAGGCAFGAUCGUCGCTT
miR-330-5p mimic *miR-NC mimic* *in-miR-330-5p* *in-miR-NC* *Bio-NC* *Bio-circPRKCA WT* *Bio-circPRKCA MUT*	UCUCUGGGCCUGUGUCUUAGGC UUUGUACUACACAAAAGUACUG GCCUAAGACACAGGCCCAGAGA UCUACUCUUUCUAGGAGGUUGGA Bio-UUUGUACUACACAAAAGUACUG Bio-UCCAGAUUAUAUCGCCCCAGAGAAAGCCAAACTTG Bio-UCCAGAUUAUAUCGGGGUCUGAAAGCCAAACTTG

Table 4 The Antibodies Used in This Study for Western Blotting and RIP

Antibody	Cat. No	Dilution
PDK1	ab110025	1:2000
p-AKT	ab38449	1:1000
AKT	ab179463	1:10,000
β-actin	ab8226	1:2500
Goat Anti-Mouse IgG H&L (HRP)	ab205719	1:10,000
Goat Anti-Rabbit IgG H&L (HRP)	ab205718	1:50,000
Ago2	ab32381	1:100
IgG	ab172730	1:200

(Millipore, Bradford, MA, USA). β-actin was detected for equal loading control.

Cell Counting Kit (CCK)-8

Cell viability was detected using CCK-8 (Yeasen, Shanghai, China) following the directions. In brief, transfected A549 and H1299 cells were inoculated in 96-well plates (2500 cells per well), and 10 μL of CCK-8 reagent was added in each well at 0, 24, 48, and 72 hours. With another incubation for 2 hours in the dark, the optical density (OD) value at 450 nm was measured on a microwell plate spectrophotometer. The reaction system of each gene was performed in quintuplicate. The cell viability curve was drawn according to OD450 values.

Transwell Assays

The migration ability and invasion ability were determined by transwell chambers (8 μm; Sigma-Aldrich, St. Louis, MO, USA) with non-coated and Matrigel-coated membrane, respectively. For both assays, A549 and H1299 cells were collected after transfection for 36 hours, and the chambers were placed in a 24-well plate. The lower space of chambers were filled with 400 μL of RPMI-1640 containing 10% FBS, and the upper spaces were filled with 200 μL of cell suspension (5×10^4 cells). This system was incubated at 37°C for another 48 hours; then, the cells on the lower surface of the chamber were fixed with 70% ethanol and stained with 0.2% crystal violet. Afterwards, the migrated cells and invaded cells were observed and counted under a microscope.

Flow Cytometry (FCM)

A549 and H1299 cells were collected after transfection for 36 hours, and the apoptosis rate was testified using Annexin V-fluorescein isothiocyanate Apoptosis Kit (Beyotime). The operation procedures were in accordance with working manual, and the cells were analyzed on FCM by sorting apoptotic cells in the Annexin V/propidium iodide (PI) quadrant. Apoptotic cells were in Annexin V +/PI+ and Annexin V+/PI- quadrants.

Bioinformatic Prediction and Dual-Luciferase Reporter Assay

The circBank (http://www.circbank.cn/searchMiRNA.html) and circinteractome (https://circinteractome.irp.nia.nih.gov/) databases were used to predict the target human miRNAs for circPRKCA. In circBank, "hsa_circ_0007580" was input in the box of "circBase ID" followed with clicking the "Search" button. In circinteractome, the "miRNA Target Sites" button was clicked, and "hsa_circ_0007580" was input in the box in Step 1 prior to clicking the "miRNA Target Sites" button in Step 3. The starBase v2.0 (http://starbase.sysu.edu.cn/starbase2/mirMrna.php) and DIANA TOOL (http://diana.imis.athena-innovation.gr/DianaTools/index.php?r=MicroT_CDS/index) databases were used to predict the target human mRNAs for miR-330-5p. In starBase v2.0, the "miRNA-mRNA interactions" button was clicked in the "miRNA-lncRNA" pull-down menu, and "has-miR-330-5p" was selected in the pull-down menu of "microRNA" prior to clicking the "Search" button. In DIANA TOOL, "has-miR-330-5p" was input in the searching box, followed with clicking the "Enter" button on the keyboard.

The wild type (WT) of circPRKCA was mutated from . . . CCCAGA . . . into . . . CGGUCU . . ., and the 3′ untranslated region (3′UTR) of PDK1 WT was mutated from . . . GGCCCAGAG . . . into CCGGGUCUC . . .. Then, circPRKCA WT and PDK1 3′UTR WT were separately cloned into pGL4 luciferase report vector, as well as their mutants (MUT). A549 and H1299 cells were co-transfected with miR-330-5p/NC mimic and circPRKCA WT/MUT or PDK1 3′UTR WT/MUT for 48 hours. The transfected cells were lysed for determination of dual-luciferase activities on GloMax®-Multi+Luminescence Module (Promega, Madison, WI, USA).

RNA Immunoprecipitation (RIP) and RNA Pull-Down Assay

For RIP, A549 and H1299 cells were transfected with miR-330-5p mimic or miR-NC mimic for 36 hours, and cell extract was obtained by RIP lysis buffer. Next, the RIP lysates were analyzed by EZ-Magna RIP Kit (Millipore)

according to the instructions. The antibodies including Ago2 and IgG were from Abcam and presented in Table 4. The expression of circPRKCA and PDK1 in RIPs was further subjected to RT-qPCR. For RNA pull-down, A549 and H1299 cells were transfected with biotinylated circPRKCA WT/MUT (Bio-circPRKCA WT/MUT) or Bio-NC, and RIP lysates were collected. The expression of miR-330-5p in circPRKCA/miRNAs/beads complexes was detected by RT-qPCR.

Xenograft Experiment

Ten BABL/c mice (male, 6-week old) were obtained from the Laboratory Animal Center of Nanjing University. A total of 4×10^6 A549 cells (in 0.2 mL of RPMI-1640 containing Matrigel) were subcutaneously injected into the right flanks of nude mice. After inoculation for 7 days, the mice were randomly divided into eight groups (n=5): si-NC, si-circPRKCA#3, si-circPRKCA#3+in-miR-NC, si-circPRKCA#3+in-miR-330-5p, miR-NC, miR-330-5p, miR-330-5p+pcDNA, and miR-330-5p+PDK1. The tumors were treated with oligonucleotides (10 nM) alone or along with vectors (0.5 μg) every 3.5 days, and tumor size (length and width) was measured every 7 days after inoculation. On the 28th day, the mice were killed and the tumors were resected; the tumor weight was measured, and tumor tissues were stored in liquid nitrogen for further total RNA and protein isolation. The animal experiment was approved by the animal care and Ethics Committee of the Yantai Yuhuangding Hospital. Animal studies were performed in compliance with the ARRIVE guidelines and the Basel Declaration. All animals received humane care according to the National Institutes of Health (USA) guidelines.

Statistical Analysis

Statistical analyses were performed using GraphPad software 7.0 (GraphPad, San Diego, CA, USA), and the data was presented as mean±standard deviation. The detection results were analyzed using two tailed Student's *t*-test and one-way analysis of variance followed by a Tukey multiple comparisons post-test. Statistical significance was set at $P<0.05$ (*), $P<0.01$ (**), $P<0.001$ (***), and $P<0.0001$ (****).

Results

CircPRKCA Was Upregulated in NSCLC Tumors and Cell Lines

According to the GSE112214 database, a cluster of circRNAs were abnormally expressed in NSCLC tumor tissues (n=3) compared to matched adjacent normal tissues (n=3), and the top eight upregulated circRNAs and down-regulated circRNAs were presented (Figure 1A). Since circPRKCA was the most upregulated one, we further confirmed its expression in a cohort of NSCLC patients (n=51) using RT-qPCR analysis. As shown in Figure 1B, expression level of circPRKCA was higher (3.1-fold, $P<0.0001$) in tumor tissues than normal tissues. Besides, the circPRKCA level was even higher in advanced NSCLC tumors (III+IV; n=30) versus that in early stages (I+II; n=21) (Figure 1C). By the way, high expression of circPRKCA was correlated with TNM stage and lymph node metastasis in this cohort of NSCLC patients (Table 1). In vitro, we validated circPRKCA expression in human NSCLC cell lines, and RT-qPCR data showed an upregulation of circPRKCA in A549 and H1299 cells paralleled with BEAS-2B cells (Figure 1D). These results demonstrated that circPRKCA was upregulated in NSCLC tumor tissues and cells, suggesting a potential oncogenic role of circPRKCA in NSCLC.

Knockdown of circPRKCA Suppressed Cell Growth, Migration, Invasion, and AKT Activity in NSCLC Cells in vitro

To further characterize the roles of circPRKCA in NSCLC, A549 and H1299 cells were exogenously silenced circPRKCA expression via siRNAs transfection. The transfection efficiency was determined by RT-qPCR, and circPRKCA level was dramatically decreased in A549 and H1299 cells transfected with special siRNAs against circPRKCA (Figure 2A and B). To obtain the optimal knockdown efficiency, si-circPRKCA#3 was selected for further functional assays. CCK-8 assay displayed an inhibition of cell viability in si-circPRKCA#3-transfected A549 and H1299 cells (Figure 2C and D). Transwell assays indicated a lowered ability of cell migration and invasion in A549 and H1299 cells administrated with si-circPRKCA#3 (Figure 2E and F). FCM revealed that the apoptosis rate of A549 and H1299 cells was elevated due to si-circPRKCA#3 introduction (Figure 2G). A great deal of evidence had revealed that the AKT signal was heavily implicated in the tumorigenesis, progression, and therapy of cancers including NSCLC.[5,24] Thus, expression of p-AKT was measured, and Western blotting manifested that relative p-AKT expression was suppressed by si-circPRKCA#3 transfection in A549 and H1299 cells (Figure 2H). These outcomes indicated a suppressive role

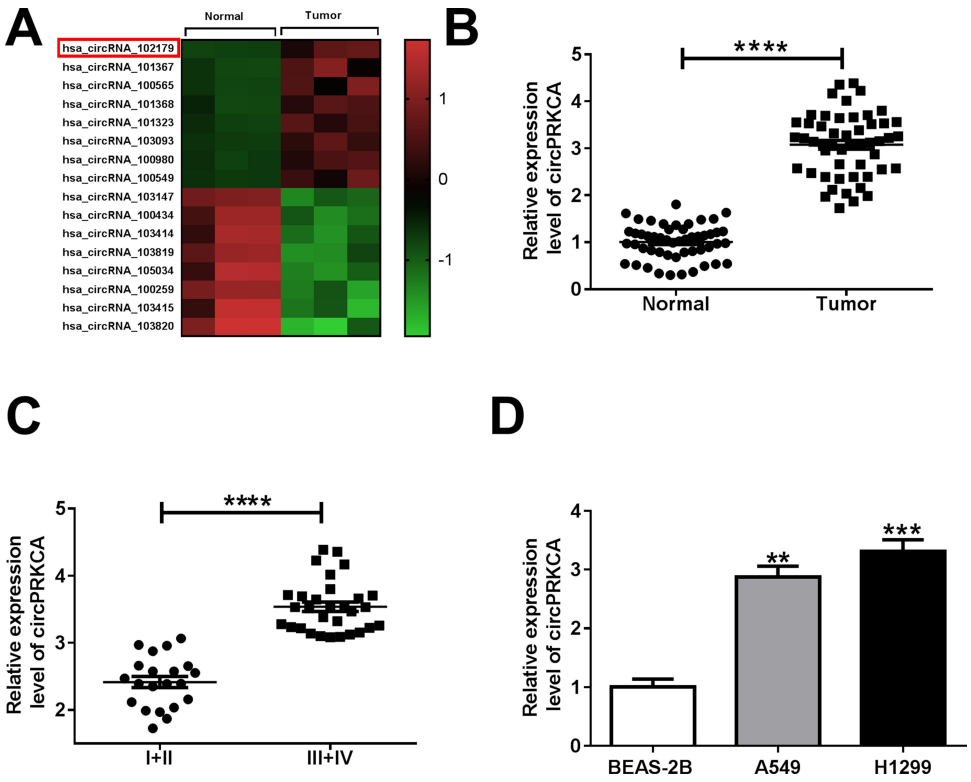

Figure 1 Circular RNA derived from human PRKCA (hsa_circPRKCA_024, circPRKCA) was upregulated in non-small-cell lung cancer (NSCLC). (**A**) GSE112214 database showed the heatmap of top eight upregulated and downregulated circRNAs in NSCLC tumor tissues (n=3; Tumor) and matched adjacent normal tissues (n=3; Normal). (**B**) RT-qPCR measured circPRKCA expression level in 51 paired human NSCLC Normal samples and Tumor samples. (**C**) RT-qPCR compared circPRKCA expression level in NSCLC tumor tissues at early stages (I+II; n=21) and advantage stages (III+IV; n=30). (**D**) RT-qPCR compared circPRKCA expression level in two human NSCLC cell lines A549 and H1299, and one normal cell line BEAS-2B. ***P*<0.01, ****P*<0.001, and *****P*<0.0001.

of circPRKCA knockdown in NSCLC cell growth, migration, invasion, and AKT activity in vitro.

CircPRKCA Targeted miR-330-5p in NSCLC Cells

One popular mechanism of circRNAs was miRNAs adsorption via target binding to participate in cellular functions. To find the target miRNAs for circPRKCA, we searched circBank (http://www.circbank.cn/searchMiRNA.html) and circinteractome (https://circinteractome/mirnasearch) databases, and a panel of six miRNAs were suggested as potential targets of circPRKCA by both databases. Therefore, the sensitivity of these miRNAs, including miR-1299, miR-197, miR-188-3p, miR-1231, miR-598, and miR-330-5p, on circPRKCA regulation was further detected; as a result, miR-330-5p was the most upregulated one in A549 and H1299 cells with circPRKCA knockdown via si-circPRKCA#3 transfection (Supplementary Figure 1A and B). Therewith, miR-330-5p was selected for further validation, and the putative binding sites of miR-330-5p on circPRKCA were mutated to the complementary binding sequences (Figure 3A). Dual-luciferase reporter system measured that the luciferase activity of vector carrying circPRKCA WT was significantly attenuated in A549 and H1299 cells transfected with miR-330-5p mimic (Figure 3B and C); whereas the luciferase activity of circPRKCA MUT vector was little affected by miR-330-5p mimic transfection. In addition, expression of circPRKCA was markedly enriched in RIP-Ago2 in A549 and H1299 cells (Figure 3D); RNA pull-down assay also showed an enrichment of miR-330-5p in the presence of Bio-circPRKCA WT instead of Bio-circPRKCA MUT (Figure 3E and F). The above results suggested a target relationship between circPRKCA and miR-330-5p in NSCLC cells. Expression of miR-330-5p was investigated using RT-qPCR, and its expression level was lower in NSCLC tumor tissues (n=51) and cell lines (A549 and H1299) than that in corresponding normal controls (Figure 3G and H). Moreover, miR-330-5p expression was increased in circPRKCA-silenced A549 and H1299 cells (Figure 3I), prompting an association of miR-330-5p upregulation and the role of circPRKCA knockdown in NSCLC.

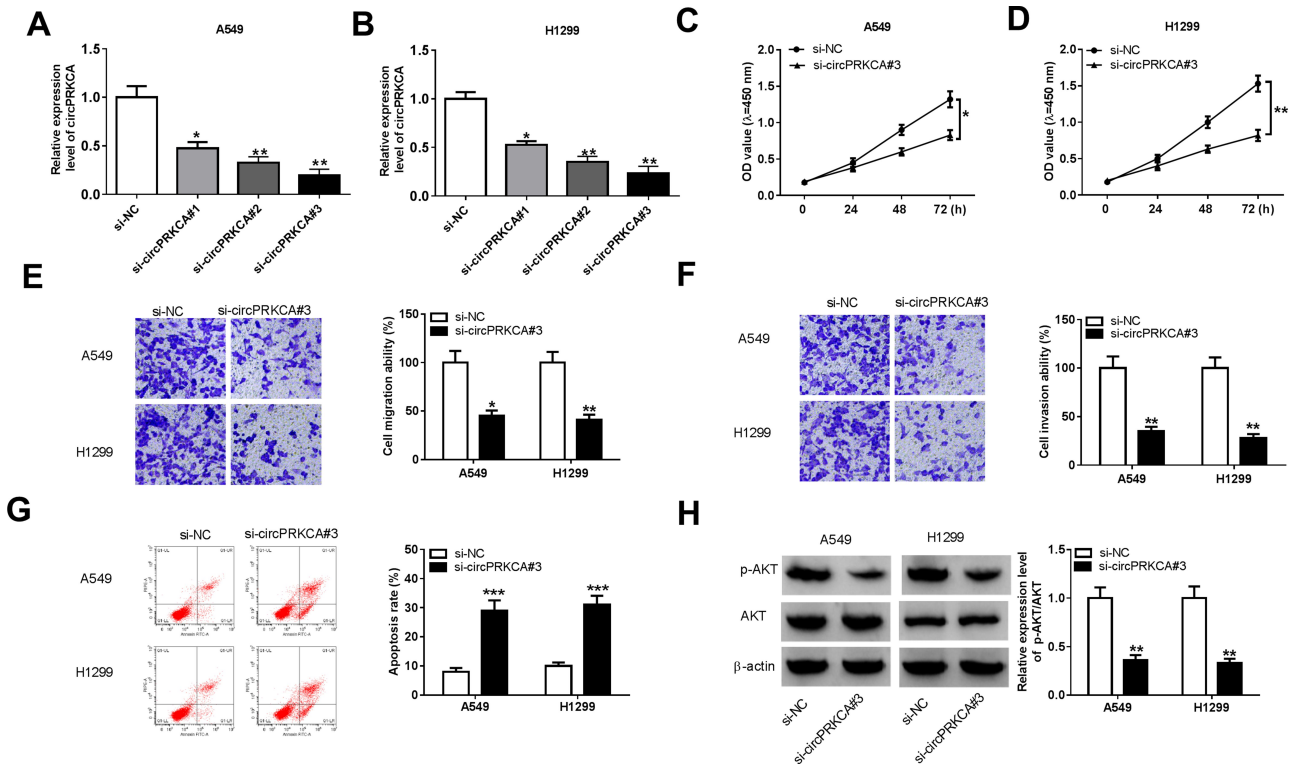

Figure 2 Functional assays of circPRKCA in NSCLC cells in vitro. (**A** and **B**) RT-qPCR detected circPRKCA expression level in A549 and H1299 cells transfected with siRNAs against circPRKCA (si-circPRKCA#1, si-circPRKCA#2, and si-circPRKCA#3) or the negative control (si-NC). (**C**–**H**) A549 and H1299 cells transfected with si-circPRKCA#3 or si-NC. (**C** and **D**) CCK-8 assay monitored cell viability at 0, 24, 48, and 72 hours. Note: OD value (λ=450 nm), the optical density at 450 nm wavelength. (**E** and **F**) Transwell assays evaluated cell migration ability (%) and invasion ability (%), and (**G**) flow cytometry (FCM) assessed apoptosis rate (%) at 36 hours. (**H**) Western blotting examined protein expression of total AKT (AKT; medium lanes) and phosphorylated AKT (p-AKT; upper lanes) at 36 hours.
Notes: p-AKT/AKT, the ratio of gray density of p-AKT blot to AKT blot. **P*<0.05, ***P*<0.01, and ****P*<0.001.

Silencing of miR-330-5p Attenuated the Suppressive Effect of circPRKCA Knockdown on Cell Growth, Migration, Invasion, and AKT Activity in NSCLC Cells in vitro

To identify the contribution of miR-330-5p in the suppressive role of circPRKCA knockdown, A549 and H1299 cells were co-transfected with si-circPRKCA#3 and in-miR-330-5p. RT-qPCR analysis showed that upregulation of miR-330-5p in circPRKCA-silenced cells was weakened by the presence of in-miR-330-5p (Figure 4A). Consequently, circPRKCA deletion-mediated suppression on cell viability (Figure 4B and C), and abilities of migration and invasion (Figure 4D and E, and Supplementary Figure 3A and B) was attenuated by miR-330-5p downregulation. On the contrary, the apoptosis rate was promoted by si-circPRKCA#3 transfection, and then was descended by in-miR-330-5p introduction (Figure 4F, and Supplementary Figure 3C). In terms of AKT activity, p-AKT expression was inhibited by circPRKCA silencing in A549 and H1299 cells, which was further abolished due to in-miR-330-5p transfection (Figure 4G). The above results identified that the suppressive role of circPRKCA knockdown in NSCLC cell growth, migration, invasion, and AKT activity was accompanied with miR-330-5p overexpression.

MiR-330-5p Targeted PDK1 3′UTR in NSCLC Cells

The downstream target of miR-330-5p in NSCLC was subsequently discovered by starBase (http://starbase.sysu.edu.cn/starbase2) and DIANA TOOL (http://DianaTools/hsa-MiR-330-5p) databases, and six common mRNAs were preliminarily selected as potential targets of miR-330-5p. Therefore, the sensitivity of these mRNAs, including protein phosphatase methylesterase 1 (PPME1), N-acetyltransferase 14 (NAT14), mediator complex subunit 15 (MED15), BTB domain containing 1 (BTBD1), ATP binding cassette subfamily E member 1 (ABCE1), and PDK1, on miR-330-5p regulation was further detected; PDK1 was the most downregulated one in

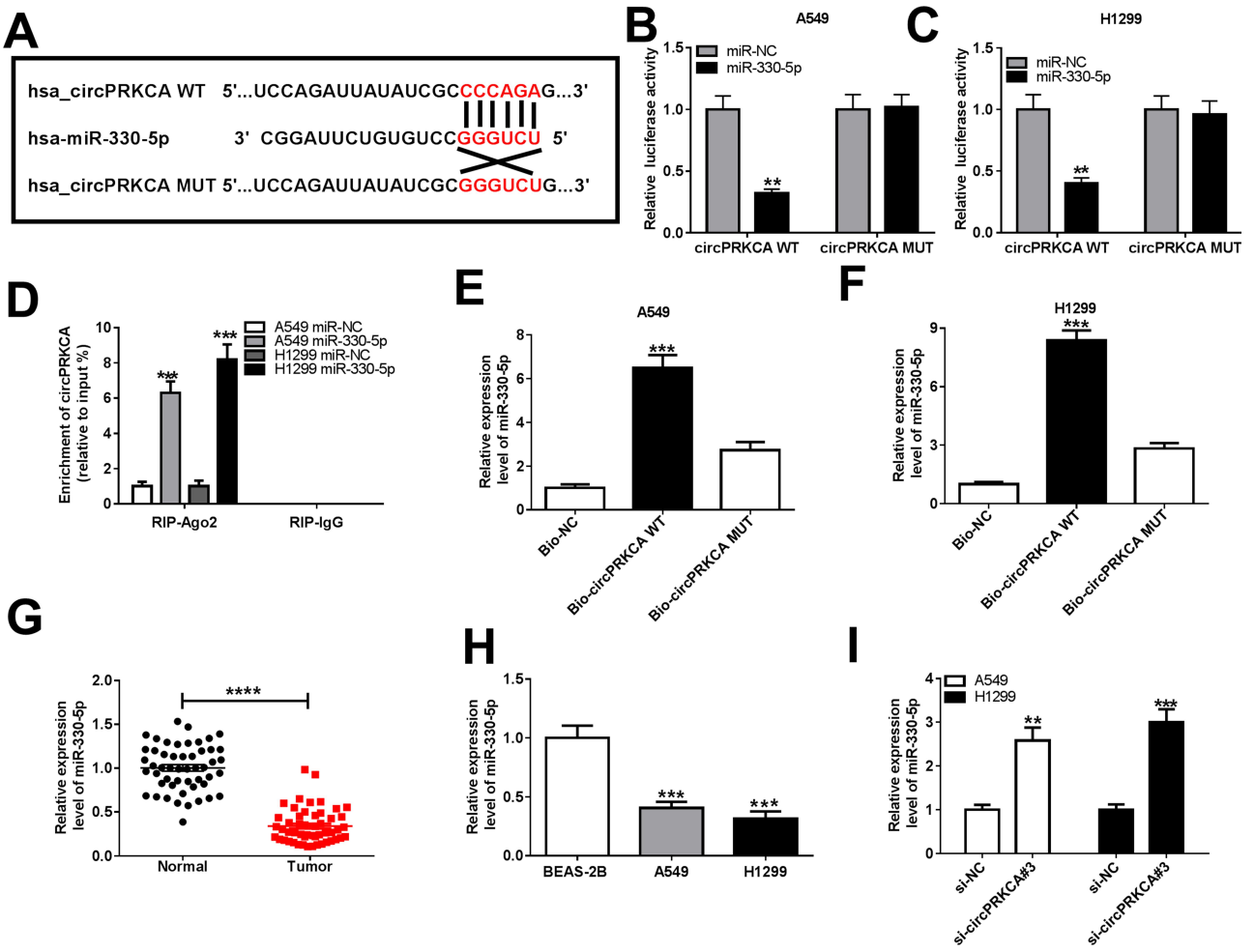

Figure 3 CircPRKCA targeted miRNA (miR)-330-5p. (**A**) The sequences between miR-330-5p and either wild type (WT) of circPRKCA or mutant (MUT) of circPRKCA. (**B** and **C**) Dual-luciferase reporter assay measured relative luciferase activity of vectors containing circPRKCA WT/MUT in A549 and H1299 cells transfected with miR-330-5p mimic (miR-330-5p) or the negative control (miR-NC). (**D**) RNA immunoprecipitation (RIP) determined the enrichment of circPRKCA in A549 and H1299 cells transfected miR-330-5p or miR-NC. Note: RIP-Ago2, RIP from Ago2 antibody; RIP-IgG, RIP from IgG antibody. (**E** and **F**) RNA pull-down assay detected miR-330-5p expression level in A549 and H1299 cells transfected with biotinylated circPRKCA WT/MUT (Bio-circPRKCA WT/MUT) or Bio-NC. (**G** and **H**) RT-qPCR measured miR-330-5p expression level in NSCLC tissues (n=51) and cell lines. (**I**) RT-qPCR confirmed miR-330-5p expression level in A549 and H1299 cells transfected with si-circPRKCA#3 or si-NC. ***P*<0.01, ****P*<0.001, and *****P*<0.0001.

A549 and H1299 cells with miR-330-5p overexpression via mimic transfection (Supplementary Figure 2A and B). Thus, PDK1 was further confirmed according to potential binding sites of miR-330-5p (Figure 5A). Dual-luciferase reporter assay and RIP assay identified this potential target relationship according to the prediction result (Figure 5B–D). Expression of PDK1 was measured using Western blotting and RT-qPCR; the protein level of PDK1 was upregulated in three tumor tissues from three randomly selected NSCLC patients and two cell lines (Figure 5E and G), and the mRNA level of PDK1 was higher in this NSCLC tumor samples (n=51) than normal samples (Figure 5F). Additionally, expression of PDK1 in A549 and H1299 cells was facilitated by in-miR-330-5p transfection, and was depressed with si-circPRKCA#3 transfection (Figure 5H and I); exogenous in-miR-330-5p could also rescue circPRKCA knockdown-mediated inhibition on PDK1 expression (Figure 5I). These results indicated that circPRKCA could regulate PDK1 expression via sponging miR-330-5p in NSCLC.

Upregulation of PDK1 Weakened the Inhibitory Effect of miR-330-5p Overexpression on Cell Growth, Migration, Invasion, and AKT Activity in NSCLC Cells in vitro

The functional experiments were performed to figure out the role of miR-330-5p and PDK1 in NSCLC cells in vitro. PDK1 expression was inhibited by miR-330-5p

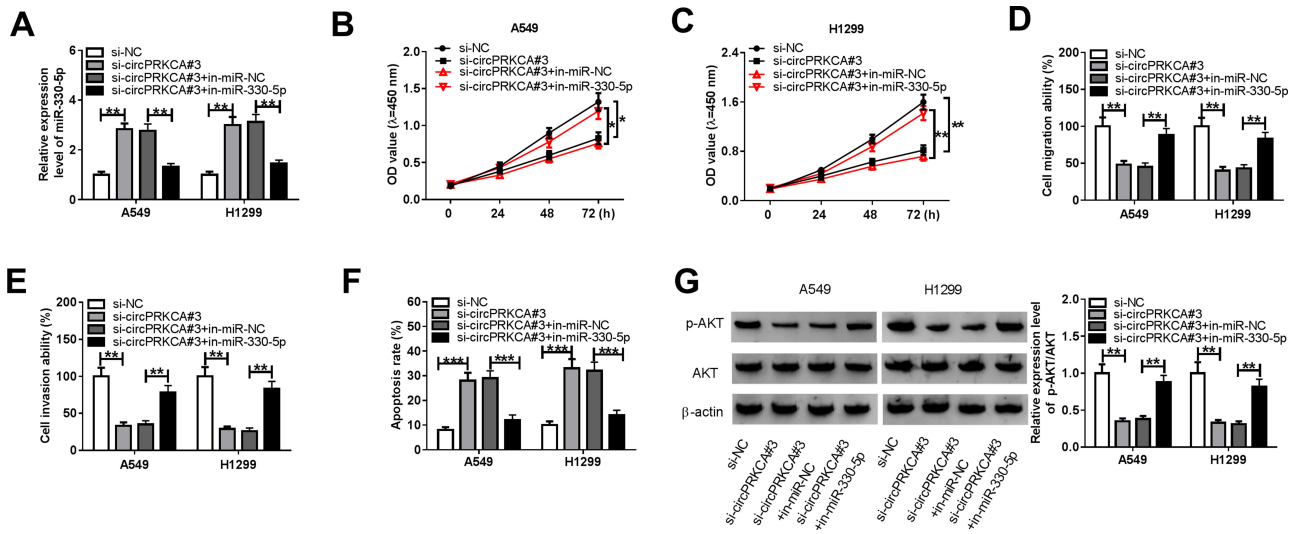

Figure 4 Functional assays of circPRKCA and miR-330-5p in NSCLC cells in vitro. (**A**) RT-qPCR detected miR-330-5p expression level in A549 and H1299 cells transfected with si-NC, si-circPRKCA#3, si-circPRKCA#3 and miR-330-5p inhibitor (in-miR-330-5p), or si-circPRKCA#3 and miR-NC inhibitor (in-miR-NC). (**B** and **C**) CCK-8 assay monitored cell viability after above transfection for 0, 24, 48, and 72 hours. (**D** and **E**) Transwell assays evaluated cell migration ability (%) and invasion ability (%), and (**F**) FCM assessed apoptosis rate (%) in above transfected A549 and H1299 cells. (**G**) Western blotting examined protein expression of AKT (medium lanes) and p-AKT (upper lanes) in A549 cells (left lanes) and H1299 cells (right lanes) after above transfection for 36 hours. **P*<0.05, ***P*<0.01, and ****P*<0.001.

mimic transfection, and this inhibition was abrogated with exogenous administration of pcDNA-PDK1 vector (PDK1) (Figure 6A). Similar to circPRKCA knockdown, miR-330-5p overexpression restrained cell viability and transwell migration and invasion abilities in A549 and H1299 cells, which was further counteracted by PDK1 restoration (Figure 6B–E, and Supplementary Figure 3D and E); contrarily, the apoptosis rate was augmented in miR-330-5p mimic-transfected A549 and H1299 cells, and then was declined by co-transfection of PDK1 (Figure 6F, and Supplementary Figure 3F); Western blotting displayed that AKT was inactivated by miR-330-5p upregulation, which was rescued in response to PDK1 upregulation, as evidenced by increased p-AKT level (Figure 6G). These data demonstrated an inhibitory role of miR-330-5p overexpression in cell viability, migration, invasion, and AKT activity in NSCLC cells in vitro depended on downregulating PDK1.

Knockdown of circPRKCA Suppressed Tumor Growth of NSCLC Cells in vivo by Regulating the miR-330-5p/PDK1/AKT Pathway

Furthermore, we launched an in-depth study to study the role of circPRKCA and miR-330-5p in xenograft tumors. The nude mice were induced tumors by subcutaneous injection of A549 cells, and si-circPRKCA#3 alone or together with in-miR-330-5p, and miR-330-5p alone or combined with PDK1 vector were used to treat these xenograft tumors. As shown in Figure 7A and E, tumor growth was restrained with si-circPRKCA#3 injection and miR-330-5p injection; tumor weight on the 28th day was less in the si-circPRKCA#3 group and miR-330-5p group (Figure 7B and F). Notably, the suppression of circPRKCA knockdown and miR-330-5p upregulation on tumor growth was counteracted by miR-330-5p downregulation and PDK1 restoration via transfections, respectively (Figure 7A–C and E–G). Consistently, expression of p-AKT was exceedingly low in tumors in the si-circPRKCA#3 group, which was abrogated with miR-330-5p injection (Figure 7D); the p-AKT expression inhibition in A549-induced xenograft tumors injected with miR-330-5p was attenuated by co-administration of the PDK1 vector (Figure 7H). These results indicated a suppressive role of circPRKCA knockdown in tumor growth in vivo through regulating the miR-330-5p/PDK1/AKT pathway.

Discussion

circRNAs were an emerging key point for disease diagnosing, treating, and inferring. Previous evidence has recently indicated that circRNAs are closely implicated in the malignant tumor progression of NSCLC.[25–27] In terms of the PI3K/AKT pathway, several circRNAs were declared to modulate this signaling pathway in NSCLC. For example, the PI3K inhibitor-LY264002

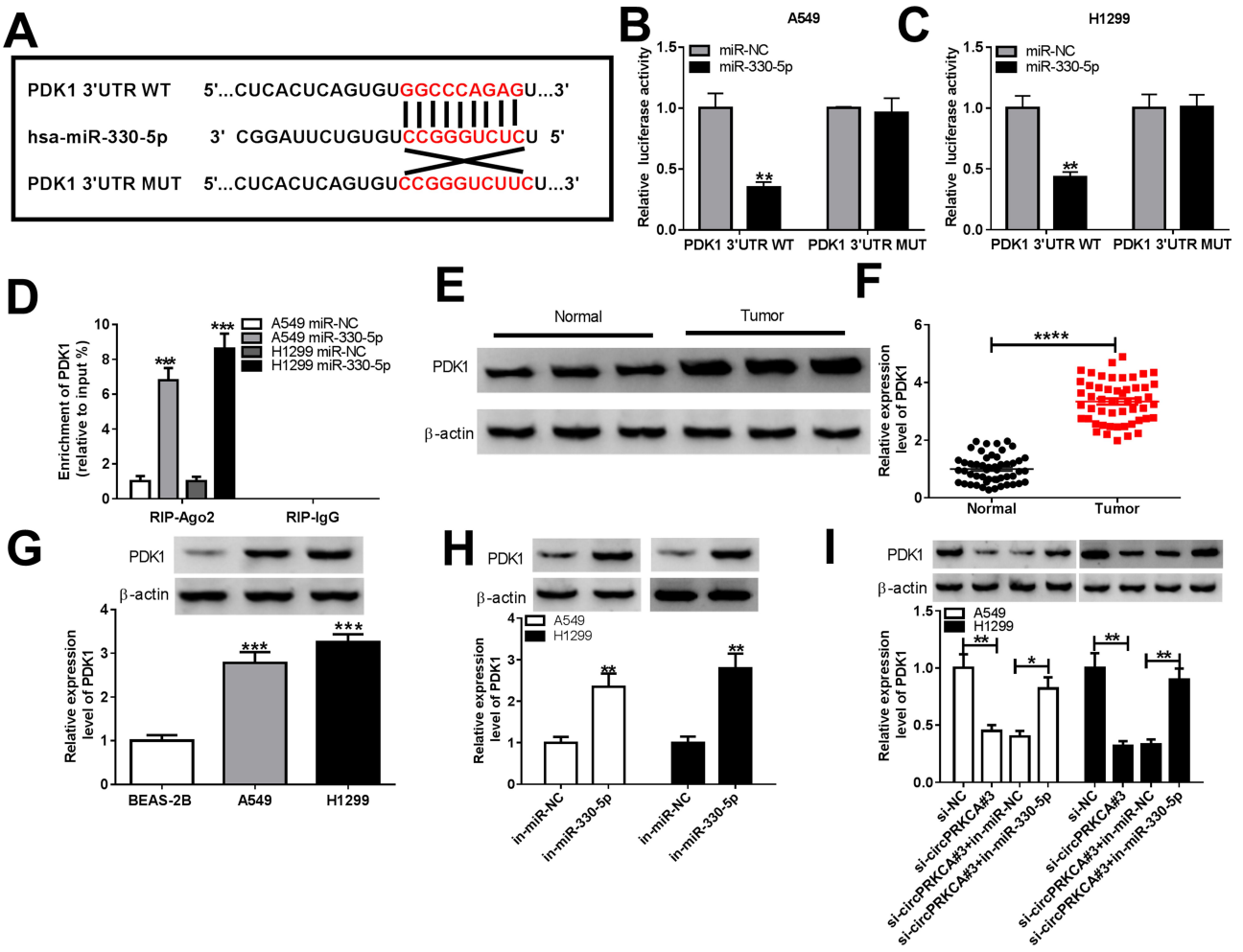

Figure 5 MiR-330-5p targeted 3′UTR of 3-phosphoinositide-dependent protein kinase-1 (PDK1). (**A**) The sequences between miR-330-5p and either wild type (WT) of PDK1 3′UTR or mutant (MUT) of PDK1 3′UTR. (**B** and **C**) Dual-luciferase reporter assay measured relative luciferase activity of vectors containing PDK1 3′UTR WT/MUT in A549 and H1299 cells transfected with miR-330-5p or miR-NC. (**D**) RIP determined the enrichment of PDK1 in A549 and H1299 cells transfected miR-330-5p or miR-NC. (**E**–**G**) Western blotting and RT-qPCR detected PDK1 expression in (**E**) three paired tissues and (**G**) 51 paired tissues from NSCLC patients, and (**G**) NSCLC cell lines. (**H** and **I**) Western blotting measured PDK1 expression level in A549 and H1299 cells transfected with (**H**) in-miR-330-5p or in-miR-NC, and (**I**) si-circPRKCA#3, si-NC, si-circPRKCA#3 and in-miR-330-5p, or si-circPRKCA#3 and in-miR-NC. **P*<0.05, ***P*<0.01, ****P*<0.001, and *****P*<0.0001.

could reverse the promoting effect of circGFRA1 overexpression on cell viability, colony formation, and expression of cyclin A1 and cyclin B1 in NSCLC cells in vitro and in vivo.[28] circFGFR3 overexpression could promote cell invasion and proliferation of 95C and H460 cells through enhancing expression of several genes, including p-AKT.[29] Abnormal expression of circRNAs in malignant pleural effusion, a common complication of lung cancer, was also elucidated by regulating several signaling pathways including PI3K-AKT and through the circRNAs-miRNAs-mRNAs network.[30] However, circRNAs involved in the PI3K/AKT pathway in NSCLC cells remained largely unclear still. Thus, in this study, we investigated the role of circPRKCA in NSCLC cell proliferation, migration, invasion, and AKT signaling via the ceRNA pathway.

Combining GSE112214 data with RT-qPCR data, we observed that circPRKCA was upregulated in NSCLC tumors and cell lines, and was associated with TNM stages. Knockdown circPRKCA could inhibit cell viability, transwell migration, and invasion abilities, as well as p-AKT expression. In vivo, circPRKCA silencing retarded tumor growth of A549 cells. The abovementioned results suggested a tumor-suppressive role of circPRKCA knockdown in NSCLC. Furthermore, miR-330-5p was confirmed to be a target of circPRKCA. To our best knowledge, this might be the first evidence to define the biologic role of circPRKCA in NSCLC cells. This could

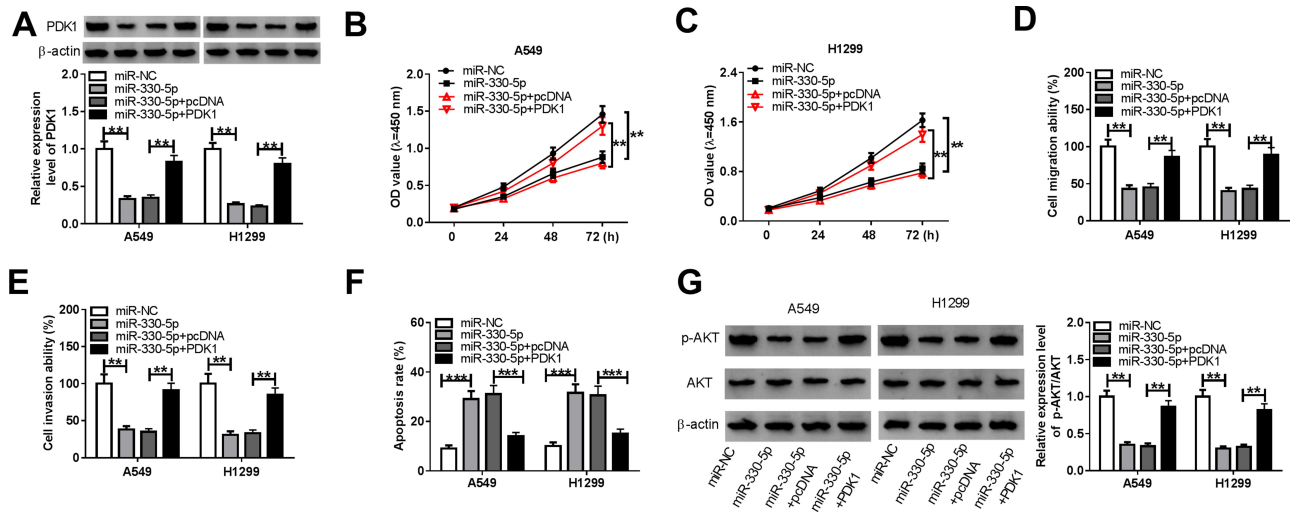

Figure 6 Functional assays of miR-330-5p and PDCK1 in NSCLC cells in vitro. (**A**) Western blotting detected PDCK1 expression level in A549 and H1299 cells transfected with miR-330-5p, miR-NC, miR-330-5p and pcDNA-PDK1 (PDK1), or miR-330-5p and pcDNA empty vector (pcDNA). (**B** and **C**) CCK-8 assay monitored cell viability of A549 and H1299 cells after above transfection for 0, 24, 48, and 72 hours. (**D** and **E**) Transwell assays evaluated cell migration ability (%) and invasion ability (%), and (**F**) FCM assessed apoptosis rate (%) in above transfected A549 and H1299 cells. (**G**) Western blotting examined protein expression of AKT (medium lanes) and p-AKT (upper lanes) in A549 cells (left lanes) and H1299 cells after (right lanes) after above transfection for 36 hours. ***P*<0.01 and ****P*<0.001.

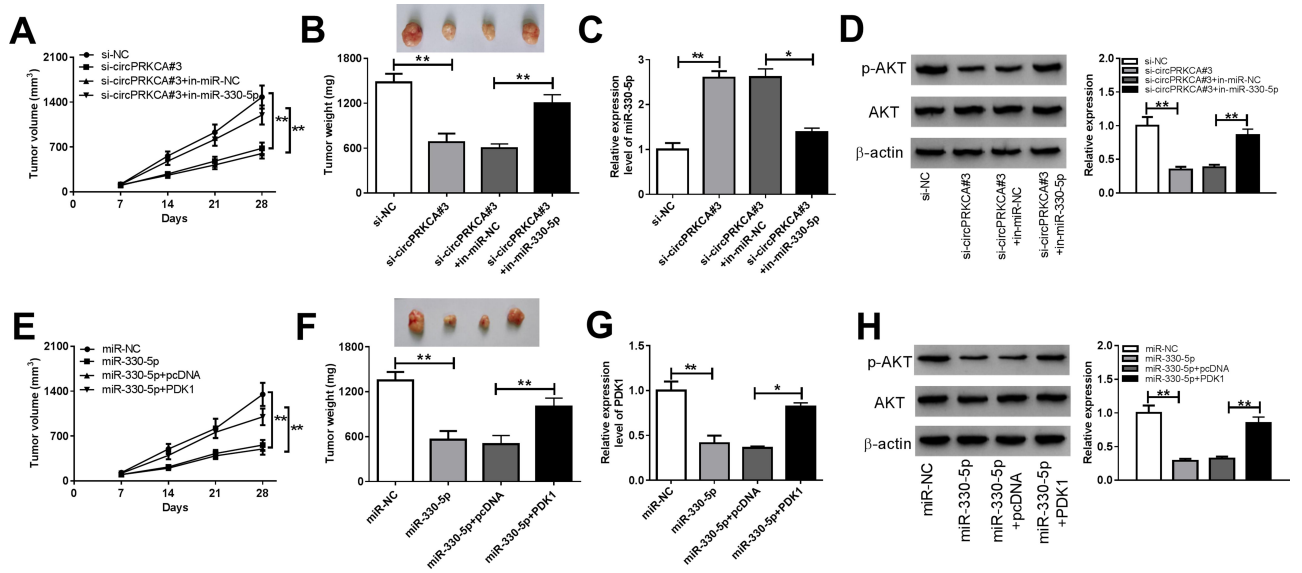

Figure 7 The role of circPRKCA, miR-330-5p, and PDK1 in cell growth of NSCLC cells in vivo via regulating AKT activity. (**A**–**H**) A549 cells were subcutaneously injected into the right flanks of nude mice, and exogenous nucleotides were injected into transplantation site (n=5) from the 7th after transplantation, including si-NC alone, and si-circPRKCA#3 alone or combined with in-miR-330-5p or in-miR-NC, miR-NC alone, and miR-330-3p alone or together with PDK1 vector or pcDNA vector. (**A** and **E**) Tumor volume was calculated every 7 days. (**B** and **F**) Tumor weight was examined on the 28th day. (**C** and **G**) RT-qPCR measured expression level of miR-330-5p and PDK1 in xenograft tumor tissues. (**D** and **H**) Western blotting detected AKT and p-AKT expression levels in xenograft tumor tissues. **P*<0.05 and ***P*<0.01.

inspire more researchers to further study this circRNA in NSCLC, and even other types of cancer.

MiR-330-5p together with miR-330-3p formed a miR-330 gene that functioned as a potential prognostic biomarker and predicted radiation sensitivity in lung cancer patients with brain metastasis.[31] Zhan et al[32] constructed a miRNA gene network including miR-330-5p contributing to the curcumin inhibition of metastasis in lung cancer A549 cells. Moreover, the cellular role of miR-330-5p was continuously clarified in NSCLC. For example, Kong et al[20] discovered that overexpression of miR-330-5p inhibited cell growth of A549 and H1299 cells by targeting NIN/RPN12 binding protein 1, as demonstrated by loss of cell viability, BrdU cell proliferation and colony formation ability, and an increase of G0/G1 arrest. Besides, miR-330-5p was linked to cancer stem cells-like properties, proliferation, migration,

and invasion by regulating;[33–36] furthermore, diverse endogenous noncoding RNAs and coding RNAs were considered as ceRNAs for this miRNA, such as lncRNAs DGCR5 and PCAT6, circRNAs circFARSA and circZKSCAN1, functional genes CD44, SOD2b, and FAM83A.[33–36] Here, we established a novel circPRKCA/miR-330-5p/PDK1 axis in NSCLC cells. And, we noticed a downregulation of miR-330-5p in NSCLC tissues and cells, which was consistent with previous studies.[20,36] The suppressive role of miR-330-5p in cell proliferation, migration, and invasion was also in favor with others.[34,36] In vivo, miR-330-5p upregulation retarded tumor growth of A549 cells. Our data demonstrated that AKT activity was also inhibited by miR-330-5p upregulation, and facilitated by miR-330-5p downregulation in NSCLC cells; the inhibition of miR-330-5p on AKT signaling was previously annotated in other cancers, such as oesophageal adenocarcinoma and colorectal cancer.[37,38] However, in lung cancer, miR-330-5p was already declared to take part in the MAPK signaling pathway.[36] However, there was little data on the association between miR-330-5p and the AKT signaling pathway prior to this present study.

PDK1 was a famous oncogene in cancers, and the PDK1/PI3K/AKT pathway had been popular in cancer malignant progression, especially in cell metastasis.[21] Here, PDK1 was overexpressed in NSCLC tissues and cells, and PDK1 downregulation was correlated with the anti-proliferation, anti-migration, and anti-invasion role of miR-330-5p in A549 and H1299 cells. In NSCLC, targeting the PDK1/PI3K/AKT pathway seemed popular in the treatment of miRNAs[39,40] and drugs.[41,42] Here, this study supported the high activation of AKT signal in NSCLC cells, accompanied with PDK1 upregulation. However, Ding et al[43] considered that miR-199a could block PDK1 expression without affecting AKT activation in NSCLC cells under hypoxia. This prompted the multiple downstream pathways under PDK1[44] and PDK1/PI3K.[45]

We might provide a novel circPRKCA/miR-330-5p/PDK1 axis in NSCLC malignant cell progression via the PDK1/AKT signaling pathway. Even though cell viability, migration, and invasion in vitro and tumor growth in vivo had been demonstrated to be affected this way, the role of the circPRKCA/miR-330-5p/PDK1 axis in many other crucial cell behaviors including cell-cycle regulation and the epithelial-mesenchymal transition remained undisclosed,[11] as well as in detail signaling pathways.[44,45] This could be new directions of circPRKCA research in NSCLC.

In conclusion, this study showed that circPRKCA was upregulated in NSCLC tumor tissues and cells, and downregulation of circPRKCA could suppress cell growth, migration, and invasion through sponging miR-330-5p and regulating the PDK1/PI3K/AKT signaling pathway.

Funding

There is no funding to report.

Disclosure of Interest

The authors declare that they have no financial or non-financial conflicts of interest for this work.

References

1. Balata H, Fong KM, Hendriks LE, et al. Prevention and early detection for NSCLC: advances in thoracic oncology 2018. *J Thorac Oncol*. 2019;14(9):1513–1527. doi:10.1016/j.jtho.2019.06.011
2. Miller KD, Nogueira L, Mariotto AB, et al. Cancer treatment and survivorship statistics, 2019. *CA Cancer J Clin*. 2019;69(5):363–385. doi:10.3322/caac.21565
3. Hirsch FR, Scagliotti GV, Mulshine JL, et al. Lung cancer: current therapies and new targeted treatments. *Lancet*. 2017;389 (10066):299–311. doi:10.1016/S0140-6736(16)30958-8
4. Mason J, Blyth B, MacManus MP, Martin OA. Treatment for non-small-cell lung cancer and circulating tumor cells. *Lung Cancer Manag*. 2017;6(4):129–139. doi:10.2217/lmt-2017-0019
5. Tan AC. Targeting the PI3K/Akt/mTOR pathway in non-small cell lung cancer (NSCLC). *Thorac Cancer*. 2020;11(3):511–518. doi:10.1111/1759-7714.13328
6. Massacesi C, Di Tomaso E, Urban P, et al. PI3K inhibitors as new cancer therapeutics: implications for clinical trial design. *Onco Targets Ther*. 2016;9:203–210. doi:10.2147/OTT.S89967
7. Perez-Ramirez C, Canadas-Garre M, Molina MA, Faus-Dader MJ, Calleja-Hernandez MA. PTEN and PI3K/AKT in non-small-cell lung cancer. *Pharmacogenomics*. 2015;16(16):1843–1862. doi:10.2217/pgs.15.122
8. Kristensen LS, Andersen MS, Stagsted LVW, Ebbesen KK, Hansen TB, Kjems J. The biogenesis, biology and characterization of circular RNAs. *Nat Rev Genet*. 2019;20(11):675–691. doi:10.1038/s41576-019-0158-7
9. Braicu C, Zimta AA, Gulei D, Olariu A, Berindan-Neagoe I. Comprehensive analysis of circular RNAs in pathological states: biogenesis, cellular regulation, and therapeutic relevance. *Cell Mol Life Sci*. 2019;76(8):1559–1577. doi:10.1007/s00018-019-03016-5
10. Su M, Xiao Y, Ma J, et al. Circular RNAs in Cancer: emerging functions in hallmarks, stemness, resistance and roles as potential biomarkers. *Mol Cancer*. 2019;18(1):90. doi:10.1186/s12943-019-1002-6
11. Li C, Zhang L, Meng G, et al. Circular RNAs: pivotal molecular regulators and novel diagnostic and prognostic biomarkers in non-small cell lung cancer. *J Cancer Res Clin Oncol*. 2019;145 (12):2875–2889. doi:10.1007/s00432-019-03045-4
12. de Fraipont F, Gazzeri S, Cho WC, Eymin B. Circular RNAs and RNA splice variants as biomarkers for prognosis and therapeutic response in the liquid biopsies of lung cancer patients. *Front Genet*. 2019;10:390. doi:10.3389/fgene.2019.00390
13. Hill KS, Erdogan E, Khoor A, et al. Protein kinase Calpha suppresses Kras-mediated lung tumor formation through activation of a p38 MAPK-TGFbeta signaling axis. *Oncogene*. 2014;33(16):2134–2144. doi:10.1038/onc.2013.147
14. Jiang H, Fu Q, Song X, et al. HDGF and PRKCA upregulation is associated with a poor prognosis in patients with lung adenocarcinoma. *Oncol Lett*. 2019;18(5):4936–4946. doi:10.3892/ol.2019.10812

15. Lahn M, Su C, Li S, et al. Expression levels of protein kinase C-alpha in non-small-cell lung cancer. *Clin Lung Cancer*. 2004;6(3):184–189. doi:10.3816/clc.2004.n.032
16. Wu KL, Tsai YM, Lien CT, Kuo PL, Hung AJ. The roles of MicroRNA in lung cancer. *Int J Mol Sci*. 2019;20(7). doi:10.3390/ijms20071611
17. Feng L, Ma J, Ji H, Liu Y, Hu W. miR-330-5p suppresses glioblastoma cell proliferation and invasiveness through targeting ITGA5. *Biosci Rep*. 2017;37(3). doi:10.1042/BSR20170019
18. Yoo HI, Kim BK, Yoon SK. MicroRNA-330-5p negatively regulates ITGA5 expression in human colorectal cancer. *Oncol Rep*. 2016;36(5):3023–3029. doi:10.3892/or.2016.5092
19. Liu DC, Song LL, Liang Q, Hao L, Zhang ZG, Han CH. Long noncoding RNA LEF1-AS1 silencing suppresses the initiation and development of prostate cancer by acting as a molecular sponge of miR-330-5p via LEF1 repression. *J Cell Physiol*. 2019;234(8):12727–12744. doi:10.1002/jcp.27893
20. Kong R, Liu W, Guo Y, et al. Inhibition of NOB1 by microRNA-330-5p overexpression represses cell growth of non-small cell lung cancer. *Oncol Rep*. 2017;38(4):2572–2580. doi:10.3892/or.2017.5927
21. Di Blasio L, Gagliardi PA, Puliafito A. Primo L. Serine/threonine kinase 3-phosphoinositide-dependent protein kinase-1 (PDK1) as a key regulator of cell migration and cancer dissemination. *Cancers (Basel)*. 2017;9(3):25. doi:10.3390/cancers9030025
22. Liu T, Yin H. PDK1 promotes tumor cell proliferation and migration by enhancing the Warburg effect in non-small cell lung cancer. *Oncol Rep*. 2017;37(1):193–200. doi:10.3892/or.2016.5253
23. Li J, Li P, Zhao W, et al. Expression of long non-coding RNA DLX6-AS1 in lung adenocarcinoma. *Cancer Cell Int*. 2015;15:48. doi:10.1186/s12935-015-0201-5
24. Song M, Bode AM, Dong Z, Lee MH. AKT as a therapeutic target for cancer. *Cancer Res*. 2019;79(6):1019–1031. doi:10.1158/0008-5472.CAN-18-2738
25. Mu Y, Xie F, Huang Y, et al. Circular RNA expression profile in peripheral whole blood of lung adenocarcinoma by high: throughput sequencing. *Medicine (Baltimore)*. 2019;98(42):e17601. doi:10.1097/MD.0000000000017601
26. Wang C, Tan S, Liu WR, et al. RNA-Seq profiling of circular RNA in human lung adenocarcinoma and squamous cell carcinoma. *Mol Cancer*. 2019;18(1):134. doi:10.1186/s12943-019-1061-8
27. Wang L, Tong X, Zhou Z, et al. Circular RNA hsa_circ_0008305 (circPTK2) inhibits TGF-beta-induced epithelial-mesenchymal transition and metastasis by controlling TIF1gamma in non-small cell lung cancer. *Mol Cancer*. 2018;17(1):140. doi:10.1186/s12943-018-0889-7
28. Yao J, Xu G, Zhu L, Zheng H. circGFRA1 enhances NSCLC progression by sponging miR-188-3p. *Onco Targets Ther*. 2020;13:549–558. doi:10.2147/OTT.S230795
29. Qiu BQ, Zhang PF, Xiong D, et al. CircRNA fibroblast growth factor receptor 3 promotes tumor progression in non-small cell lung cancer by regulating Galectin-1-AKT/ERK1/2 signaling. *J Cell Physiol*. 2019;234(7):11256–11264. doi:10.1002/jcp.27783
30. Wen Y, Wang Y, Xing Z, Liu Z, Hou Z. Microarray expression profile and analysis of circular RNA regulatory network in malignant pleural effusion. *Cell Cycle*. 2018;17(24):2819–2832. doi:10.1080/15384101.2018.1558860
31. Hodzic J, Giovannetti E, Diosdado B, Adema AD, Peters GJ. Regulation of deoxycytidine kinase expression and sensitivity to gemcitabine by micro-RNA 330 and promoter methylation in cancer cells. *Nucleosides Nucleotides Nucleic Acids*. 2011;30(12):1214–1222. doi:10.1080/15257770.2011.629271
32. Zhan JW, Jiao DM, Wang Y, et al. Integrated microRNA and gene expression profiling reveals the crucial miRNAs in curcumin anti-lung cancer cell invasion. *Thorac Cancer*. 2017;8(5):461–470. doi:10.1111/1759-7714.12467
33. Wang R, Dong HX, Zeng J, Pan J, Jin XY. LncRNA DGCR5 contributes to CSC-like properties via modulating miR-330-5p/CD44 in NSCLC. *J Cell Physiol*. 2018;233(9):7447–7456. doi:10.1002/jcp.26590
34. Cui LH, Xu HR, Yang W, Yu LJ. lncRNA PCAT6 promotes non-small cell lung cancer cell proliferation, migration and invasion through regulating miR-330-5p. *Onco Targets Ther*. 2018;11:7715–7724. doi:10.2147/OTT.S178597
35. Hang D, Zhou J, Qin N, et al. A novel plasma circular RNA circFARSA is a potential biomarker for non-small cell lung cancer. *Cancer Med*. 2018;7(6):2783–2791. doi:10.1002/cam4.1514
36. Wang Y, Xu R, Zhang D, et al. Circ-ZKSCAN1 regulates FAM83A expression and inactivates MAPK signaling by targeting miR-330-5p to promote non-small cell lung cancer progression. *Transl Lung Cancer Res*. 2019;8(6):862–875. doi:10.21037/tlcr.2019.11.04
37. Bibby BA, Reynolds JV, Maher SG. MicroRNA-330-5p as a putative modulator of neoadjuvant chemoradiotherapy sensitivity in oesophageal adenocarcinoma. *PLoS One*. 2015;10(7):e0134180. doi:10.1371/journal.pone.0134180
38. Mansoori B, Mohammadi A, Naghizadeh S, et al. miR-330 suppresses EMT and induces apoptosis by downregulating HMGA2 in human colorectal cancer. *J Cell Physiol*. 2020;235(2):920–931. doi:10.1002/jcp.29007
39. Wei Y, Liao Y, Deng Y, Zu Y, Zhao B, Li F. MicroRNA-503 inhibits non-small cell lung cancer progression by targeting PDK1/PI3K/AKT pathway. *Onco Targets Ther*. 2019;12:9005–9016. doi:10.2147/OTT.S213059
40. Wang Y, Zhang Z, Wang H, et al. miR-138-1* regulates aflatoxin B1-induced malignant transformation of BEAS-2B cells by targeting PDK1. *Arch Toxicol*. 2016;90(5):1239–1249. doi:10.1007/s00204-015-1551-4
41. Liu R, Chen Z, Yi X, et al. 9za plays cytotoxic and proapoptotic roles and induces cytoprotective autophagy through the PDK1/Akt/mTOR axis in non-small-cell lung cancer. *J Cell Physiol*. 2019;234(11):20728–20741. doi:10.1002/jcp.28679
42. Wang R, Zhang Q, Peng X, et al. Stellettin B Induces G1 arrest, apoptosis and autophagy in human non-small cell lung cancer A549 cells via blocking PI3K/Akt/mTOR pathway. *Sci Rep*. 2016;6:27071. doi:10.1038/srep27071
43. Ding G, Huang G, Liu HD, et al. MiR-199a suppresses the hypoxia-induced proliferation of non-small cell lung cancer cells through targeting HIF1alpha. *Mol Cell Biochem*. 2013;384(1–2):173–180. doi:10.1007/s11010-013-1795-3
44. Gagliardi PA, Puliafito A, Primo L. PDK1: at the crossroad of cancer signaling pathways. *Semin Cancer Biol*. 2018;48:27–35. doi:10.1016/j.semcancer.2017.04.014
45. Lien EC, Dibble CC, Toker A. PI3K signaling in cancer: beyond AKT. *Curr Opin Cell Biol*. 2017;45:62–71. doi:10.1016/j.ceb.2017.02.007